

# Extreme quantum nonlinearity in superfluid thin-film surface waves

Yasmine L. Sfindla<sup>\*1</sup>, Christopher G. Baker<sup>1</sup>, Glen I. Harris<sup>1</sup>, Lin Tian<sup>2</sup>, and Warwick P. Bowen<sup>1</sup>

<sup>\*</sup>Corresponding author: [y.sfindla@uqconnect.edu.au](mailto:y.sfindla@uqconnect.edu.au)

<sup>1</sup>*ARC Centre of Excellence for Engineered Quantum Systems, School of Mathematics and Physics, The University of Queensland, Brisbane 4072, Australia*

<sup>2</sup>*School of Natural Sciences, University of California, Merced, California 95343, USA*

(Dated: May 28, 2020)

We show that highly confined superfluid films are extremely nonlinear mechanical resonators, offering the prospect to realize a mechanical qubit. Specifically, we consider third-sound surface waves, with nonlinearities introduced by the van der Waals interaction with the substrate. Confining these waves to a disk, we derive analytic expressions for the cubic and quartic nonlinearities and determine the resonance frequency shifts they introduce. We predict single-phonon shifts that are three orders of magnitude larger than in current state-of-the-art nonlinear resonators. Combined with the exquisitely low intrinsic dissipation of superfluid helium, we predict that this could allow blockade interactions between phonons as well as two-level-system-like behavior. Our work provides a new pathway towards extreme mechanical nonlinearities, and towards quantum devices that use mechanical resonators as qubits.

## INTRODUCTION

Nonlinearities are widely used in quantum technologies. For instance, they allow the generation of nonclassical states [1–6], two-qubit interactions [7–9], and quantum nondemolition measurements [10–14]. Sufficiently strong nonlinearities can introduce resolvable anharmonicity in a resonator, so that when resonantly driven it can only absorb a single quantum of energy, mimicking the behavior of a two-level system. This provides the possibility of blockade-type interactions, where phonons (or photons, depending on the resonator) can only pass through the resonator one at a time [15–17] and it allows artificial qubits to be engineered, such as the superconducting qubits widely used in quantum computing [18].

Nonlinear *mechanical* resonators have quantum applications ranging from the preparation of nonclassical states [19–22] to quantum-enhanced force sensing [23–27], quantum backaction-evading measurement [28], and mechanical quantum state tomography [29]. Achieving the single-phonon nonlinear regime in a mechanical resonator is of both fundamental and technological importance. It would allow artificial atoms to be built from massive objects consisting of billions of atoms, testing quantum physics in uncharted regimes of macroscopicity, and would provide a new form of qubit for quantum computation among other quantum applications [17, 30].

Reaching the single-phonon nonlinear regime in a mechanical resonator requires an intrinsic nonlinearity far stronger than what has been achieved to date [31–37], combined with exceptionally low dissipation so that the energy level shifts introduced by the nonlinearity are resolvable. Here, we propose to achieve this in a resonator constructed from a thin spatially confined superfluid helium film, similar to the ones used in recent experimental work on optomechanical cooling [38], lasing [39] and quantized vortex detection [40]. The use of superfluid helium affords exceptionally low intrinsic dissipation [41], and we show here that the van der Waals interaction with the substrate introduces strong nonlinearities.

We derive an analytical model of the cubic and quartic (Duffing) nonlinearities due to van der Waals forces for a film confined on a circular disk. We find that the quartic nonlinearity depends strongly on the radius of the disk, and predict that the nonlinearity in a 5 nm thick film with 100 nm radius would manifest single-phonon frequency shifts three orders of magnitude larger than those seen in state-of-the-art nonlinear mechanical resonators including graphene sheets [36], carbon nanotubes [36] and molecule-coupled resonators [37]. With submillihertz dissipation rates observed in third-sound resonators, albeit of millimeter dimensions [41], this level of nonlinearity could allow the single-phonon nonlinear regime to be reached.

The cubic nonlinearity is large as well. However,

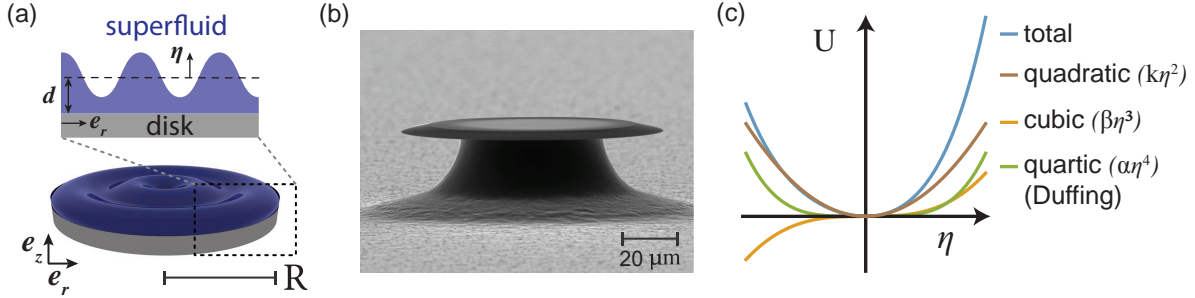


Figure 1: (a) Illustration of a surface wave of amplitude  $\eta[r, \theta]$  in a thin superfluid helium film of mean thickness  $d$ , confined to a circular geometry of radius  $R$ . (b) Previously demonstrated experimental methods for circular confinement of a superfluid helium film include adsorption of the film on the surface of an on-chip microdisk as shown in this SEM micrograph [38–40, 42], or on the inside of parallel disks of a capacitor as in Ref. [43, 44]. (c) Anharmonic potential of a superfluid oscillator with spring constant  $k$ , cubic nonlinear constant  $\beta$  and quartic (Duffing) constant  $\alpha$ .

it is nonresonant in the system’s Hamiltonian and therefore its impact on the mechanical resonance frequency is suppressed. Previous work on classical mechanical resonators has shown that its primary effect is to modify the magnitude of the quartic nonlinearity [45–47]. Our numerical simulations show that this result extends to quantum resonators, so long as they are not far within the single-phonon nonlinear regime. All together, we conclude surface waves in thin superfluid helium may be an ideal macroscopic candidate to achieve the single-phonon nonlinear regime in a mechanical resonator—and through this, to probe quantum macroscopicity and build a new class of qubits for quantum computing and metrology.

## RESULTS

### I. The anharmonic superfluid oscillator

Superfluid helium has a combination of traits often sought after in mechanical resonators: low mechanical dissipation arising from near-zero viscosity, and ultralow optical absorption. Indeed, it has been used as the mechanical resonator in several recent optomechanical platforms [38, 39, 42, 48–54] and in experiments that study the physics of quantum fluids [40, 55]. In these references, the superfluid fills a cavity [50–52] or channel [53], is levitated as a droplet [49], or spread out as a few-nanometers-thin film [38, 39, 41, 56]. The latter case is investigated here. The thin film exhibits thickness fluctuations that resemble shallow water waves, as illustrated in Fig. 1a. The waves are named “third sound” and are unique to two-dimensional superfluid helium films [41, 56, 57].

In this work, we consider the superfluid film to be

confined to a circular surface of radius  $R$ . This geometry is quite general, and can be realized for instance by condensing the film on the surface of a microscopic silica disk (see Fig. 1b) [38, 39, 42, 58]. That design is attractive because it allows laser light to circulate in the disk. These “whispering-gallery” light waves interact strongly with the third-sound waves in the superfluid, and can serve as a tool to observe and control the superfluid motion [38]. In this study however, we focus on the film’s dynamics: while constrained here to a circular disk, we expect our predictions to be qualitatively mirrored in other superfluid thin-film geometries.

A helium atom at height  $z$  is attracted to the substrate atoms via the van der Waals force [59, 60]. This leads to a height-dependent potential energy per unit mass stored in a film, given by

$$V[z] = -\frac{a_{\text{vdw}}}{z^3}, \quad (1)$$

with  $a_{\text{vdw}}$  the substrate-dependent van der Waals coefficient characterizing the attraction strength [59], which provides a restoring force for fluctuations of the film surface. Turning to Fig. 1a, the circularly confined film somewhat resembles a drumhead—and in fact, the helium surface undulates like the skin of a resonating drum. While it is clear that Eq. (1) is nonlinear and therefore does not describe a Hookean potential, in the small amplitude limit (where nonlinearities can be neglected) the resonances of the surface can be described by Bessel modes [58]. The time-dependent mode amplitude  $h[r, \theta, t]$  that quantifies the deviation of the film height from the mean thickness  $d$  with polar coordinates  $r$  and  $\theta$  is given by [58]

$$h[r, \theta, t] = \eta[r, \theta] \sin(\Omega_m t) \quad (2)$$

with

$$\eta[r, \theta] = A J_\mu \left[ \zeta_{\mu, \nu} \frac{r}{R} \right] \cos(\mu \theta). \quad (3)$$

Here,  $A$  is the amplitude,  $J_\mu$  is the Bessel function of the first kind of integer order  $\mu$ , and  $\Omega_m = (\zeta_{\mu, \nu} c_3)/R$  is the mechanical resonance frequency in the absence of nonlinearity. Here the resonance frequency depends on the superfluid speed of sound  $c_3 = \sqrt{3a_{\text{vdw}} d^{-3}}$  and a parameter  $\zeta_{\mu, \nu}$ , which depends on the boundary conditions. In the absence of flow across the resonator boundary, the film is described by *volume-conserving* Bessel modes, i.e., Bessel functions with free boundary conditions [58]. These mode amplitudes have an extremum at  $r = R$ : a condition met by choosing  $\zeta_{\mu, \nu}$  as the  $\nu^{\text{th}}$  zero of  $J'_\mu$ . Hence,  $\eta[r, \theta]$  is the time-independent amplitude of a drumhead mode typically specified by its mode numbers  $(\mu, \nu)$  with the order  $\mu$  the number of nodal diameters, also called *azimuthal mode number* (i.e.,  $2\mu$  is the number of zeros in the azimuthal direction for  $\theta = 0$  to  $2\pi$ ) and  $\nu$  the number of nodal circles, also called *radial mode number* (i.e.,  $\nu$  is the number of zeros in the radial direction for  $r = 0$  to  $R$ ). The Bessel mode function  $J_\mu \left[ \zeta_{\mu, \nu} \frac{r}{R} \right]$  is graphed in Fig. 2, and the values  $\zeta_{\mu, \nu}$  for the first three mode numbers are tabulated in Table 1.

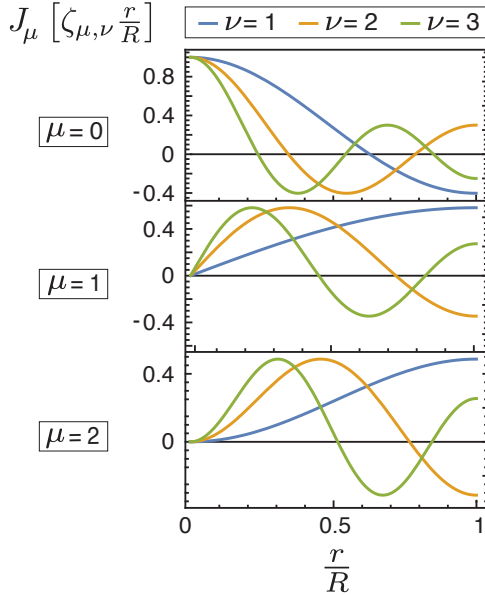


Figure 2: Bessel modes with free boundary conditions  $J_\mu \left[ \zeta_{\mu, \nu} \frac{r}{R} \right]$  of (azimuthal) orders  $\mu = 0, 1$  and  $2$ , for radial mode number  $\nu = 1$  to  $3$ .

While these eigenmodes are, strictly speaking, valid only for a linear oscillator, they are a good approximation for the high quality (see Sec. III) mechanical resonances considered here where the nonlin-

	$\zeta_{\mu, \nu}$		
	$\nu = 1$	$\nu = 2$	$\nu = 3$
$\mu = 0$	3.83	7.02	10.2
$\mu = 1$	1.84	5.33	8.54
$\mu = 2$	3.05	6.71	9.97

Table 1: The first three roots ( $\nu = 1$  to  $3$ ) of the derivative of the Bessel function  $J'_\mu$  [61].

earity only shifts the mechanical resonance frequency by a small fraction.

The van der Waals potential energy stored in the surface deformation  $U$  is obtained by integrating the potential  $V$  over the deviation from equilibrium and introducing the superfluid density  $\rho$  [58]:

$$U = \rho \int_0^{2\pi} \int_0^R \int_d^{d+\eta[r, \theta]} V[z] r dr d\theta dz \quad (4)$$

With Eq. (1) and the Taylor series expansion, we obtain

$$\begin{aligned} \int_d^{d+\eta[r, \theta]} V[z] dz &= \frac{a_{\text{vdw}}}{2} \left( \frac{1}{(d + \eta[r, \theta])^2} - \frac{1}{d^2} \right) \\ &= \frac{a_{\text{vdw}}}{2d^2} \sum_{j=0}^{\infty} (j+2) \left( -\frac{\eta[r, \theta]}{d} \right)^{j+1}. \end{aligned} \quad (5)$$

Previous work on linear superfluid optomechanics only considered the first two terms in this expansion [58] while the higher-order terms were omitted. In the present work, we cast light on these higher-order nonlinear terms. The first term (proportional to  $\eta$ ) averages out to zero for volume-conserving Bessel modes with  $\int_r \int_\theta \eta[r, \theta] = 0$ . The third- and fourth-order terms respectively represent cubic and quartic nonlinearities. We neglect terms of fifth order in  $\eta$  and higher, expecting them to be small compared to these first two nonlinear terms. Thus, Eq. (4) becomes

$$\begin{aligned} U = \rho \int_0^{2\pi} \int_0^R \left( \underbrace{\frac{3 a_{\text{vdw}} \eta^2[r, \theta]}{2 d^4}}_{\text{linear spring}} - \underbrace{\frac{2 a_{\text{vdw}} \eta^3[r, \theta]}{d^5}}_{\text{quadratic spring}} \right. \\ \left. + \underbrace{\frac{5 a_{\text{vdw}} \eta^4[r, \theta]}{2 d^6}}_{\text{cubic spring}} \right) r dr d\theta, \end{aligned} \quad (7)$$

where we have identified the quadratic, cubic and quartic potential energies associated with linear,

quadratic and cubic spring terms.<sup>1</sup> By introducing a reference point  $x := \eta[R, 0]$ —that is, the displacement at the periphery of the disk at an angular location  $\theta = 0$ —we can rewrite the potential energy as

$$U = \frac{1}{2}kx^2 + \frac{1}{3}\beta x^3 + \frac{1}{4}\alpha x^4. \quad (8)$$

This is the potential energy of an anharmonic oscillator (see Fig. 1c) with restoring force  $F = -\nabla U = -kx - \beta x^2 - \alpha x^3$ , where  $k$  is the linear spring constant given by

$$k = \frac{3\rho a_{\text{vdw}}}{d^4} \int_0^{2\pi} \int_0^R \frac{\eta^2[r, \theta]}{\eta^2[R, 0]} r \, dr \, d\theta, \quad (9)$$

and  $\beta$  and  $\alpha$  are the nonlinear spring constants. The *cubic nonlinearity* is given by

$$\beta = -\frac{6\rho a_{\text{vdw}}}{d^5} \int_0^{2\pi} \int_0^R \frac{\eta^3[r, \theta]}{\eta^3[R, 0]} r \, dr \, d\theta \quad (10)$$

and the *quartic* (also known as *Duffing*) *nonlinearity* is given by

$$\alpha = \frac{10\rho a_{\text{vdw}}}{d^6} \int_0^{2\pi} \int_0^R \frac{\eta^4[r, \theta]}{\eta^4[R, 0]} r \, dr \, d\theta. \quad (11)$$

By evaluating the integrals (see Supplementary Information), the strong dependence of the (non)linear spring constants on the film thickness  $d$  and confinement radius  $R$  is exposed:

$$k = (1 + \delta_{\mu 0}) 3\pi \rho a_{\text{vdw}} \phi_{\mu, \nu}^{(2)} \frac{R^2}{d^4} \quad (12)$$

$$= (1 + \delta_{\mu 0}) \frac{3\pi}{2} \rho a_{\text{vdw}} \left(1 - \frac{\mu^2}{\zeta_{\mu, \nu}^2}\right) \frac{R^2}{d^4}, \quad (13)$$

$$\beta = -\delta_{\mu 0} 12\pi \rho a_{\text{vdw}} \phi_{0, \nu}^{(3)} \frac{R^2}{d^5} \quad (14)$$

and

$$\alpha = (3 + 5\delta_{\mu 0}) \frac{5\pi}{2} \rho a_{\text{vdw}} \phi_{\mu, \nu}^{(4)} \frac{R^2}{d^6}. \quad (15)$$

Here we have introduced the Kronecker delta function  $\delta$ , and integrals of the Bessel function  $\phi_{\mu, \nu}^{(p)} := \frac{\int_0^{\zeta_{\mu, \nu}} J_{\mu}^p[q] q \, dq}{\zeta_{\mu, \nu}^2 J_{\mu}^p[\zeta_{\mu, \nu}]}$  for  $p = \{2, 3, 4\}$  tabulated in Table 2.

The film thickness  $d$  can be independently determined and tuned in situ, as we demonstrated in previous work [38], while the confinement radius  $R$  can

<sup>1</sup>In this work we label the nonlinearities by the orders in which they appear as energies and potentials, because we work exclusively in the Hamiltonian formalism. In some other work, especially early work on spring forces, they may be labeled by their (lower) order in force and acceleration equations.

be changed through choice of device geometry. By controlling these, Eq. (14) and (15) reveal that it is possible to access a wide range of cubic and quartic nonlinearities.

It is worth noting that the cubic nonlinearity  $\beta$  vanishes for all but the rotationally invariant ( $\mu = 0$ ) modes, but otherwise, the linear and nonlinear constants alike depend—through the constants  $\phi_{\mu, \nu}^{(p)}$ —only marginally on the mode numbers  $\mu$  and  $\nu$  (see Supplementary Information).

Although the relationships found here suggest that the nonlinear coefficients are larger for thinner films and larger radii, the desired parameter regime depends on the relative magnitude of the nonlinear and linear coefficients, and the mass. In the following section, we will derive what exactly that regime is and what platform parameters one should aim for, in order to reach it.

$\phi_{\mu, \nu}^{(2)}$			
	$\nu = 1$	$\nu = 2$	$\nu = 3$
$\mu = 0$	1/2	1/2	1/2
$\mu = 1$	0.353	0.482	0.493
$\mu = 2$	0.286	0.456	0.480
$\phi_{\mu, \nu}^{(3)}$			
$\mu = 0$	-0.437	0.259	-0.236
$\phi_{\mu, \nu}^{(4)}$			
$\mu = 0$	1.28	1.48	1.61
$\mu = 1$	0.290	0.837	1.03
$\mu = 2$	0.223	0.704	0.891

Table 2: Coefficients  $\phi_{\mu, \nu}^{(p)} = \frac{\int_0^{\zeta_{\mu, \nu}} J_{\mu}^p[q] q \, dq}{\zeta_{\mu, \nu}^2 J_{\mu}^p[\zeta_{\mu, \nu}]}$  for  $p = \{2, 3, 4\}$  with  $\zeta_{\mu, \nu}$  the  $\nu^{\text{th}}$  zero of the Bessel function  $J_{\mu}$ .

## II. The quartic (Duffing) potential

From Eq. (8), the Hamiltonian for the oscillator with natural frequency  $\Omega_m$ , effective mass  $m_{\text{eff}}$ , spring constant  $k = m_{\text{eff}} \Omega_m^2$  and zero-point fluctuation amplitude  $x_{\text{zpf}} = \sqrt{\hbar/2m_{\text{eff}} \Omega_m}$  reads:

$$H = \frac{p^2}{2m_{\text{eff}}} + \frac{1}{2}kx^2 + \frac{1}{3}\beta x^3 + \frac{1}{4}\alpha x^4 \quad (16)$$

$$= \hbar\Omega_m \left(n + \frac{1}{2}\right) + \frac{x_{\text{zpf}}^3}{3}\beta(a + a^\dagger)^3 + \frac{x_{\text{zpf}}^4}{4}\alpha(a + a^\dagger)^4$$

with  $a$  ( $a^\dagger$ ) the phonon annihilation (creation) operators satisfying the commutation relation  $[a, a^\dagger] = 1$ ,

the canonical position and momentum operators  $x$  and  $p$  satisfying  $x = x_{\text{zpf}}(a + a^\dagger)$  and  $[x, p] = i\hbar$ , and  $n = a^\dagger a$  the phonon number.

Because the nonlinear terms are much smaller than the linear term in the potential energy, we treat the nonlinear terms as perturbations to the Hamiltonian of the harmonic oscillator and use a perturbation-theory approach to derive the corrections of the eigenenergies due to the nonlinear terms. Under the perturbation theory, the cubic nonlinear term—constituting only non-energy-conserving transitions—adds no first-order contribution to the eigenenergies [62]. Similarly, by expanding the quadratic nonlinear term, we have:

$$\begin{aligned} (a + a^\dagger)^4 &= a^2 a^{\dagger 2} + a^\dagger a^2 a^\dagger + (a a^{\dagger 2})^2 \\ &\quad + \underbrace{a^4 + a^2 a^\dagger a + a^3 a^\dagger + a a^\dagger a^2 + a^\dagger a^3}_{\text{non-energy-conserving}} + \text{h.c.} \\ &= 6n^2 + 6n + 3 + \dots \end{aligned} \quad (17)$$

Hence to the first order of the perturbation theory, the energy eigenvalues of the Fock states of the harmonic oscillator become

$$E_n = \hbar \left( \Omega_m + \frac{3x_{\text{zpf}}^4 \alpha}{2\hbar} \right) \left( n + \frac{1}{2} \right) + \hbar \frac{3x_{\text{zpf}}^4 \alpha}{2\hbar} n^2. \quad (18)$$

These eigenenergies describe an oscillator with energy levels that are shifted in proportion to the phonon number  $n$  (see Fig. 3a). The quartic (Duffing) nonlinearity therefore shifts the transition frequency between the  $n = 0$  and  $n = 1$  states by

$$\delta\Omega_m^0 := \frac{3}{2} \frac{x_{\text{zpf}}^4 \alpha}{\hbar}. \quad (19)$$

With this definition, Eq. (18) can be rewritten as

$$E_n = \hbar (\Omega_m + (n+1)\delta\Omega_m^0) n + \hbar \frac{\Omega_m + \delta\Omega_m^0}{2} n^2. \quad (20)$$

Thus, in the frequency spectrum of the oscillator (see Fig. 3b) resonances signaling single-phonon transitions between states  $n$  and  $n+1$  appear at frequencies

$$\Omega[n] := \frac{E_{n+1} - E_n}{\hbar} = \Omega_m + 2(n+1)\delta\Omega_m^0, \quad (21)$$

each separated by a frequency difference  $2\delta\Omega_m^0$ . When the mechanical decay rate (or linewidth)  $\Gamma$  of

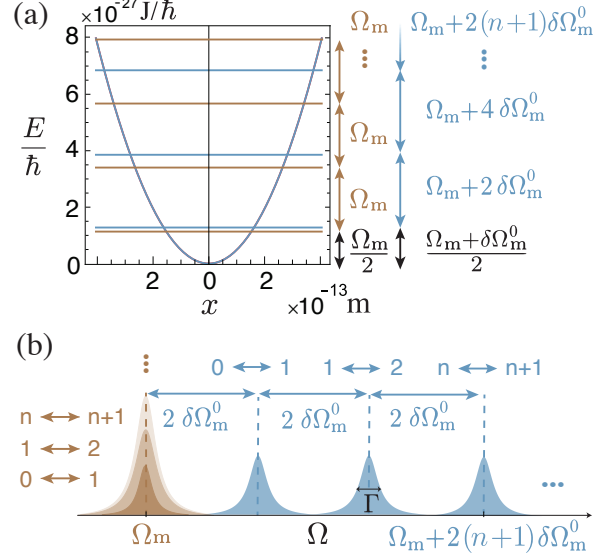


Figure 3: (a) Energy spectrum (analytical solutions) for  $R = 0.5 \mu\text{m}$ ,  $d = 10 \text{ nm}$  of a linear (beige) and nonlinear (blue) resonator, with energy shifts enlarged by a factor  $10^8$  to facilitate visual representation. (b) Illustration of the corresponding single-phonon transition frequencies. The harmonic oscillator features only a single resonance at  $\Omega_m$  (beige); the anharmonic oscillator (blue) exhibits degenerate spectral features at  $\Omega[n] = \Omega_m + 2(n+1)\delta\Omega_m^0$ .

the oscillator is smaller than the spectral splitting, i.e.,

$$\Gamma < 2\delta\Omega_m^0, \quad (22)$$

the single-phonon transitions are resolved and the intrinsic granularity of the oscillator's energy is revealed, as in the experiments in Ref. [1] and [2] where an ancillary system provided the required nonlinearity. We term this the *single-phonon nonlinear regime*: the regime where a single phonon shifts the resonance frequency by more than the linewidth. In this regime, the resonator is sufficiently anharmonic that a single absorbed phonon shifts the frequency off resonance for phonons that arrive later: it behaves more like a two-level system than an harmonic oscillator. Alternatively, when one introduces a critical amplitude

$$x_{\text{crit}} := \sqrt{\frac{2}{3} \frac{m_{\text{eff}} \Gamma \Omega_m}{\alpha}} \quad (23)$$

as in Ref. [37], one could say that the single-phonon nonlinear regime is reached if the zero-point fluctuation amplitude exceeds the critical amplitude:  $x_{\text{zpf}} > x_{\text{crit}}$ .

Using Eq. (12) to (15) we can express  $x_{\text{zpf}}^4 \alpha$  in

terms of the adjustable parameters  $R$  and  $d$ . With

$$x_{\text{zpf}} = \sqrt{\frac{\hbar}{(1 + \delta_{\mu 0})\pi\sqrt{3}a_{\text{vdw}}\rho\left(1 - \frac{\mu^2}{\zeta_{\mu,\nu}^2}\right)}} \zeta_{\mu,\nu}^{\frac{1}{2}} \frac{d^{\frac{5}{4}}}{R^{\frac{3}{2}}} \quad (24)$$

one obtains

$$\delta\Omega_{\text{m}}^0 = (3 - \delta_{\mu 0}) \frac{5\hbar}{4\pi\rho} \frac{\phi_{\mu,\nu}^{(4)}}{\left(1 - \frac{\mu^2}{\zeta_{\mu,\nu}^2}\right)^2} \frac{\zeta_{\mu,\nu}^2}{R^4 d}. \quad (25)$$

This expression identifies every parameter available to the researcher who seeks to maximize the single-phonon nonlinear strength of the superfluid resonator: the shift grows drastically with decreasing confinement radius  $R$ , scales with the inverse of the film thickness  $d$ , but is independent of the van der Waals coefficient  $a_{\text{vdw}}$  between the helium film and the substrate. The shift is always positive, so the oscillator is effectively “spring-hardened”.

Its dependence on the mode numbers  $(\mu; \nu)$  is rather intricate due to the lack of a closed form of the coefficients  $\zeta_{\mu,\nu}$  and  $\phi_{\mu,\nu}^{(4)}$  (see Supplementary Information). Therefore, we have graphed the frequency shift as a function of the mode numbers  $(\mu; \nu)$  in Fig. 4. It can be seen that the nonlinear strength  $\delta\Omega_{\text{m}}^0$  can grow by four orders of magnitude when the Bessel mode order  $\mu$  and radial mode number  $\nu$  vary from 0 (for the mode order) and 1 (for the radial mode number) to 20.

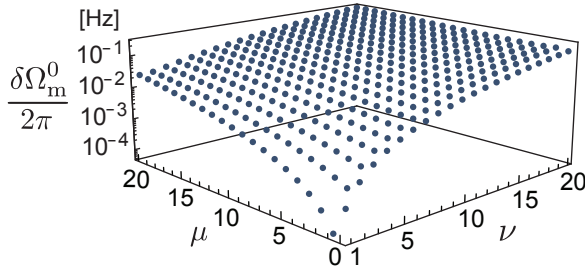


Figure 4: Resonance frequency shift induced by a single phonon,  $\delta\Omega_{\text{m}}^0 = 3\alpha x_{\text{zpf}}^4 / 2\hbar$ , as function of the Bessel mode order  $\mu$  and radial node number  $\nu$  for a 5 nm thick superfluid film confined to a 1  $\mu\text{m}$  radius, assuming a pure Duffing nonlinearity ( $\beta = 0$ ).

The predicted nonlinearity of the superfluid film is compared to other systems in Table 3 for a range of confinement radii  $R$  and radial nodes  $\nu$ . From the table it is clear that the *simultaneous* attainment of large  $\alpha$  and  $x_{\text{zpf}}$  is nontrivial for many platforms, while for the superfluid third-sound resonator both are intrinsically large and tunable. When a 5 nm thick superfluid film is confined to a radius

of 10  $\mu\text{m}$ , its predicted single-phonon frequency shift surpasses those in membranes [31], cantilevers [32], and  $\text{Si}_3\text{N}_4$  beams [33–35]. For  $R = 1 \mu\text{m}$ , it exceeds levitated nanoparticles that inherit their strong nonlinearity from an optical trapping potential [63] and resonators with an engineered chemical bond [37]. Finally, in the submicron regime, single-phonon nonlinear shifts might surpass those of carbon nanotubes and graphene sheets [36] by orders of magnitude, overshooting the single-phonon nonlinear threshold.

### III. Reaching the single-phonon nonlinear regime in confined thin superfluid helium

Having obtained the parameter space required to bring a thin-film superfluid resonator into the single-phonon nonlinear regime, the question becomes: Are there platforms available that may facilitate these requirements? Can one reasonably engineer an on-chip superfluid resonator whose damping  $\Gamma$  approaches the single-phonon frequency shift  $\delta\Omega_{\text{m}}^0$ ?

In the earliest third-sound resonators [43, 44], the superfluid film was adsorbed on the inside of two parallel metalized silica disks. This approach allowed capacitive detection of the film’s dynamics: film thickness variations change the capacitance between the plates. In previous works, we have used a few-nanometers-thick film adsorbed on a single on-chip silica microdisk allowing optical detection of the film’s dynamics: film thickness variations change the index of refraction encountered by whispering-gallery light waves [38–40, 42]. Unfortunately, glass disks become unsuitable for confinement below  $\sim 10 \mu\text{m}$  micron. Using high refractive index materials such as silicon or gallium arsenide instead, the disks can be miniaturized down to  $\sim 1 \mu\text{m}$  radii [64]. These setups span region (b) in Fig. 5; it can be seen that reaching the single-phonon nonlinear regime then requires damping rates in the millihertz regime. This is a challenging condition, yet such low damping rates—with corresponding mechanical quality factors  $Q = \Omega_{\text{m}}/\Gamma$  in excess of  $10^5$ —have been experimentally observed in Ref. [41], albeit for larger millimeter dimensions.

Further size reduction could be achieved through the use of hybrid phononic-photonic crystal cavities: capillary forces in superfluid helium [51] would naturally fill the holes of a photonic crystal membrane [65], leading to a periodic modulation of the speed of sound experienced by a superfluid third-sound wave. Thereby, they could enable confinement from hundreds to tens of nanometers (Fig. 5a). Such an approach also presents the advantage of potentially ultralow mechanical dissipation by virtue of a super-

Class	Resonator	Nonlinearity	$\alpha$ [ $\frac{\text{N}}{\text{m}^3}$ ]	$x_{\text{zpf}}$ [m]	$\frac{2\delta\Omega_m^0}{2\pi}$ [Hz]	$\frac{\Omega_m}{2\pi}$ [Hz]	$m_{\text{eff}}$ [kg]	$\frac{\Gamma}{2\pi}$ [Hz]	$\frac{2\delta\Omega_m^0}{\Gamma}$	Year	Ref.
Superfluid	Third sound (R=100 nm, d=5 nm, $\nu = 10$ )	Intrinsic	$3 \times 10^{16}$	$2 \times 10^{-12}$	$8 \times 10^2$	$4 \times 10^8$	$9 \times 10^{-21}$				
Superfluid	Third sound (R=100 nm, d=5 nm, $\nu = 1$ )	Intrinsic	$2 \times 10^{16}$	$5 \times 10^{-13}$	7	$5 \times 10^7$	$6 \times 10^{-19}$				
Bottom-up resonator	Graphene sheet	Intrinsic	$2 \times 10^{16}$	$3 \times 10^{-13}$	$9 \times 10^{-1}$	$2 \times 10^8$	$4 \times 10^{-19}$	$4 \times 10^4$	$2 \times 10^{-5}$	2011	[36]
Bottom-up resonator	Carbon nanotube	Intrinsic	$6 \times 10^{12}$	$2 \times 10^{-12}$	$3 \times 10^{-1}$	$3 \times 10^8$	$8 \times 10^{-21}$	$5 \times 10^3$	$7 \times 10^{-5}$	2011	[36]
Superfluid	Third sound (R=1 $\mu\text{m}$ , d=5 nm, $\nu = 10$ )	Intrinsic	$3 \times 10^{18}$	$5 \times 10^{-14}$	$8 \times 10^{-2}$	$4 \times 10^7$	$9 \times 10^{-17}$				
MEMS	Gold-covered d.c. Si beam	Chemical bond	$1 \times 10^{20}$	$7 \times 10^{-15}$	$1 \times 10^{-3}$	$2 \times 10^6$	$1 \times 10^{-13}$	$5 \times 10^2$	$3 \times 10^{-6}$	2016	[37]
Superfluid	Third sound R=1 $\mu\text{m}$ , d=5 nm, $\nu = 1$ )	Intrinsic	$2 \times 10^{18}$	$2 \times 10^{-14}$	$7 \times 10^{-4}$	$5 \times 10^6$	$6 \times 10^{-15}$				
Levitated particle	Levitated silica nanoparticle	Optical trap	$-1 \times 10^7$	$5 \times 10^{-12}$	$3 \times 10^{-5}$	$1 \times 10^5$	$3 \times 10^{-18}$	$8 \times 10^{-4}$	$4 \times 10^{-2}$	2017	[63]
Superfluid	Third sound (R=10 $\mu\text{m}$ , d=5 nm, $\nu = 10$ )	Intrinsic	$3 \times 10^{20}$	$2 \times 10^{-15}$	$8 \times 10^{-6}$	$4 \times 10^6$	$9 \times 10^{-13}$				
NEMS	Metallized SiC beam	Intrinsic	$5 \times 10^{14}$	$4 \times 10^{-14}$	$6 \times 10^{-6}$	$9 \times 10^6$	$6 \times 10^{-16}$	$1 \times 10^3$	$5 \times 10^{-9}$	2006	[47]
NEMS	D.c. Si <sub>3</sub> N <sub>4</sub> beam	Qubit	$8 \times 10^{15}$	$2 \times 10^{-14}$	$5 \times 10^{-6}$	$6 \times 10^7$	$4 \times 10^{-16}$	$1 \times 10^3$	$4 \times 10^{-9}$	2010	[35]
Levitated particle	Levitated particle	Optical trap	$-8 \times 10^3$	$2 \times 10^{-11}$	$2 \times 10^{-6}$	$7 \times 10^4$	$5 \times 10^{-19}$	$6 \times 10^2$	$3 \times 10^{-9}$	2019	[67]
Superfluid	Third sound (R=10 $\mu\text{m}$ , d=5 nm, $\nu = 1$ )	Intrinsic	$2 \times 10^{20}$	$5 \times 10^{-16}$	$7 \times 10^{-8}$	$5 \times 10^5$	$6 \times 10^{-11}$				
NEMS	D.c. four-layer piezoelectric beam	Intrinsic	$8 \times 10^{14}$	$9 \times 10^{-15}$	$3 \times 10^{-8}$	$1 \times 10^7$	$1 \times 10^{-14}$	$1 \times 10^4$	$2 \times 10^{-12}$	2013	[68]
NEMS	D.c. Si beam	Intrinsic	$5 \times 10^{13}$	$1 \times 10^{-14}$	$1 \times 10^{-8}$	$5 \times 10^7$	$8 \times 10^{-16}$	$8 \times 10^3$	$1 \times 10^{-12}$	2016	[69]
NEMS	D.c. Si <sub>3</sub> N <sub>4</sub> /Nb bilayer beam	Intrinsic	$2 \times 10^{11}$	$4 \times 10^{-14}$	$1 \times 10^{-9}$	$1 \times 10^6$	$7 \times 10^{-15}$	$2 \times 10^1$	$9 \times 10^{-11}$	2014	[34]
MEMS	Suspended InP membrane	Intrinsic	$4 \times 10^{13}$	$9 \times 10^{-15}$	$1 \times 10^{-9}$	$1 \times 10^6$	$1 \times 10^{-13}$	$2 \times 10^2$	$6 \times 10^{-12}$	2013	[31]
NEMS	D.c. Si <sub>3</sub> N <sub>4</sub> beam	Intrinsic	$1 \times 10^{10}$	$3 \times 10^{-14}$	$4 \times 10^{-11}$	$9 \times 10^5$	$1 \times 10^{-14}$	2	$3 \times 10^{-11}$	2018	[33]
MEMS	Metallic plate Casimir resonator	Intrinsic	$3 \times 10^9$	$6 \times 10^{-15}$	$1 \times 10^{-14}$	$2 \times 10^3$	$1 \times 10^{-10}$	$3 \times 10^{-1}$	$5 \times 10^{-14}$	2001	[70]
AFM	Commercial van der Waals cantilever	Intrinsic	$2 \times 10^9$	$4 \times 10^{-15}$	$3 \times 10^{-15}$	$4 \times 10^4$	$1 \times 10^{-11}$	$1 \times 10^3$	$2 \times 10^{-18}$	2002	[32]

Table 3: Overview of nonlinearities in various systems, sorted in order of decreasing single-phonon nonlinear frequency splitting  $2\delta\Omega_m^0 = \frac{3\alpha x_{\text{zpf}}^4}{\hbar}$ . Tabulated values for third sound (highlighted) use rotationally invariant modes ( $\mu = 0$ ) with superfluid density  $\rho = 145 \text{ kg/m}^3$  and the van der Waals coefficient for silica  $a_{\text{vdw}} = 2.65 \times 10^{-24} \text{ m}^5 \text{ s}^{-2}$  [71]. Tabulated numbers are for pure Duffing nonlinearities ( $\beta = 0$ ). For the third-sound resonators, higher-order contributions from a cubic nonlinearity ( $\beta \neq 0$ ) reduces the effective Duffing nonlinearity to respectively  $0.6\alpha$  and  $0.98\alpha$  for  $\nu = 1$  and 10: see Sec. IV.

D.c.: doubly clamped.



fluid phononic bandgap [66], and could put the challenging single-phonon nonlinear regime within reach.

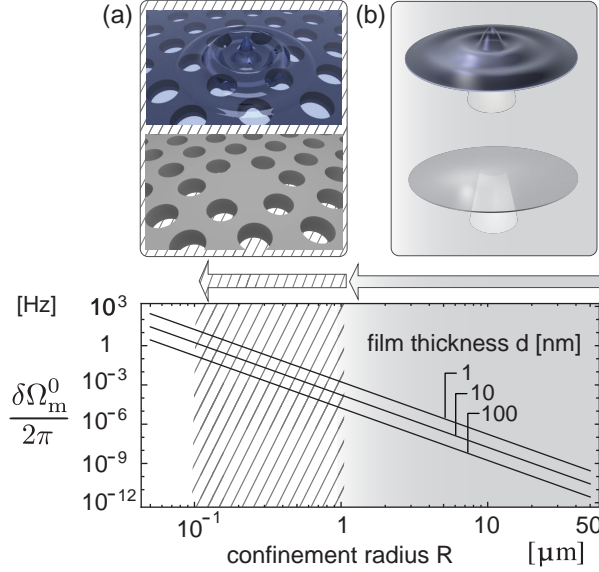


Figure 5: Resonance frequency shift induced by a single phonon  $\delta\Omega_m^0 = 3\alpha x_{zpf}^4/2\hbar$  as a function of mode confinement radius for various superfluid film thicknesses  $d$  for the  $(\mu = 0; \nu = 1)$  mode, assuming a pure Duffing nonlinearity ( $\beta = 0$ ). The quantized nature of the anharmonic oscillator energy spectrum is resolvable if the mechanical linewidth  $\Gamma < 2\delta\Omega_m^0$ . Insets: (a) confinement radii achievable through phononic crystal lattice trapping, (b) confinement radii for microdisks [38–40, 42].

#### IV. Effect of the cubic potential

The analysis thus far only contains the first-order correction of the resonator energy by the nonlinear terms, to which the cubic potential energy does not contribute. However, the cubic nonlinearity  $\beta$  found in Eq. (14) is substantial. Such significant cubic nonlinearities are not unique to superfluid resonators: they are common in general mechanical resonators with high-quartic nonlinearities like nanobeams and cantilevers, membranes and graphene sheets [45]. It is therefore broadly important to understand their effect on the dynamics of quantum-Duffing oscillators, and whether they influence the ability to reach the single-phonon nonlinear regime.

We model the effect of the cubic nonlinearity  $\beta$  in the quantum regime by comparing numerical solutions of the full Hamiltonian to an analytical approximation rooted in the classical theory of Duffing

resonators. Previous work [45–47] on quartic and cubic nonlinearities in the classical regime suggests that the cubic potential can be absorbed into the quartic Duffing potential, giving rise to an effective quartic nonlinearity  $\alpha_{\text{eff}}[\alpha, \beta]$  where

$$\alpha_{\text{eff}} = \alpha - \frac{10}{9} \frac{\beta^2}{k}. \quad (26)$$

We reiterate here that we found in Eq. (14) that only rotationally invariant ( $\mu = 0$ ) modes have a nonzero cubic nonlinearity  $\beta \neq 0$ . Substituting the superfluid spring constants from Eq. (12) to (15) yields the following expression:

$$\frac{\alpha_{\text{eff}}}{\alpha} = 1 - \frac{10}{9} \frac{\beta^2}{k\alpha} = 1 - \delta_{\mu 0} \frac{8}{3} \frac{(\phi_{0,\nu}^{(3)})^2}{\phi_{0,\nu}^{(4)}}. \quad (27)$$

Remarkably, the effective modification of the Duffing nonlinearity by a cubic nonlinearity  $\beta$  depends uniquely on the number of radial nodes  $\nu$ . Furthermore, as  $\nu$  increases,  $\alpha_{\text{eff}}$  rapidly approaches  $\alpha$ . Indeed, since

$$\lim_{\nu \rightarrow \infty} \frac{(\phi_{0,\nu}^{(3)})^2}{\phi_{0,\nu}^{(4)}} = \frac{0}{\infty} = 0,$$

we have in the limit of large  $\nu$

$$\lim_{\nu \rightarrow \infty} \frac{\alpha_{\text{eff}}}{\alpha} = 1, \quad (28)$$

and for the  $(\mu = 0; \nu = 1)$  mode,  $\alpha_{\text{eff}} = 0.6\alpha$  while for a  $(\mu = 0; \nu = 10)$  mode  $\alpha_{\text{eff}} = 0.98\alpha$ .

In Ref. [45], the approximation (26) was derived in the regime where the average Duffing force is at least a factor of  $Q^{-1}$  smaller than the average linear force. Hence, we must have  $k\bar{x} > \alpha\bar{x}^3/Q$  for an oscillator displacement  $\bar{x}$ . That can be written as  $\sqrt{m_{\text{eff}}\Omega_m\Gamma/\alpha} > \bar{x}$ , with on the left hand side  $\sqrt{\frac{3}{2}}$  the critical amplitude  $x_{\text{crit}}$  we introduced in Eq. (23), i.e.,  $\sqrt{\frac{3}{2}}x_{\text{crit}} > \bar{x}$ . The parameter regime for validity of both Eq. (26) and single-phonon resolution  $x_{zpf} > x_{\text{crit}}$ , hence requires that  $x_{zpf} > \bar{x}$ . This requirement cannot be satisfied for phonon Fock states where  $\bar{x} \leq x_{zpf}$ . Therefore, it is unclear whether the approximation can be directly applied to the single-phonon nonlinear regime.

From Section III, the single-phonon nonlinear regime that might be practically achievable with a third-sound resonator is  $1 < 2\delta\Omega_m^0/\Gamma < 1000$ , which we will term the *mid quantum regime*. To test whether the approximation is applicable in this



regime, we use the Lindblad-master-equation formalism of open quantum systems. Specifically, we numerically solve the Lindblad master equation for a resonator with cubic and quartic nonlinearities (see Supplementary Information).

We compare the resulting correlation spectra  $S_{xx}$  for three cases: a superfluid resonator with finite quartic and cubic nonlinearity  $S_{xx}[\alpha, \beta]$ , a pure Duffing resonator  $S_{xx}[\alpha, 0]$ , and a pure Duffing resonator with an effective quartic strength  $S_{xx}[\alpha_{\text{eff}}, 0]$  conform to Eq. (27). They are shown, for a range of single-photon nonlinear strengths  $2\delta\Omega_m^0/\Gamma$ , in Fig. 6.

It is evident at a glance that as the single-phonon nonlinear strength  $2\delta\Omega_m^0/\Gamma$  exceeds unity, the nonlinearity lifts the oscillator's spectral degeneracy—and with it, the veil on its inherent quantized nature. The spectra for pure Duffing resonators  $S_{xx}[\alpha, 0]$  manifest transition resonances<sup>2</sup> at the values  $\Omega[n] = \Omega_m + 2(n+1)\delta\Omega_m^0[\alpha]$  obtained analytically from first-order perturbation theory. The pure Duffing spectrum does, however, differ significantly from the full-Hamiltonian third-sound resonator spectrum  $S_{xx}[\alpha, \beta]$ , and from that of the effective Duffing third-sound resonator  $S_{xx}[\alpha_{\text{eff}}, 0]$ . The latter two are nearly identical in all cases, both in terms of amplitude and transition resonance frequencies. This indicates that, even though the system resides outside the regime for which the approximation of Eq. (26) has been shown to be classically valid, it appears to be a good approximation here. I.e., the third-sound resonator with a quadratic nonlinearity  $\beta$  appears to be accurately described by the effective Duffing resonator according to Eq. (27), and its single-phonon transition frequencies are correctly analytically predicted as  $\Omega[n] = \Omega_m + 2(n+1)\delta\Omega_m^0[\alpha_{\text{eff}}]$  from Eq. (19).

All together, we conclude that within the mid quantum regime—where emerging intrinsically nonlinear resonators are expected to operate—a nonresonant cubic potential can be included in the Hamiltonian as a partial reduction of the quartic nonlinearity  $\alpha$ , although further work is required to support these numerical observations with a rigorous theoretical foundation. For the thin-film resonator, the reduced single-phonon shift is uniquely dependent on the film's radial node number according to Eq. (27): the influence of the cubic nonlinearity rapidly diminishes for modes with increasing numbers of radial nodes.

<sup>2</sup>The small discrepancy stems from the numerical error on the bare energy eigenstates  $E_n$ , which increases with  $n$ . This absolute error is inversely proportional to the size of the basis spanning the Hilbert space in the numerical algorithm; the smaller  $\alpha$  and  $\delta\Omega_m^0$ , the larger the basis must be chosen to mitigate the relative error on the transition frequencies.

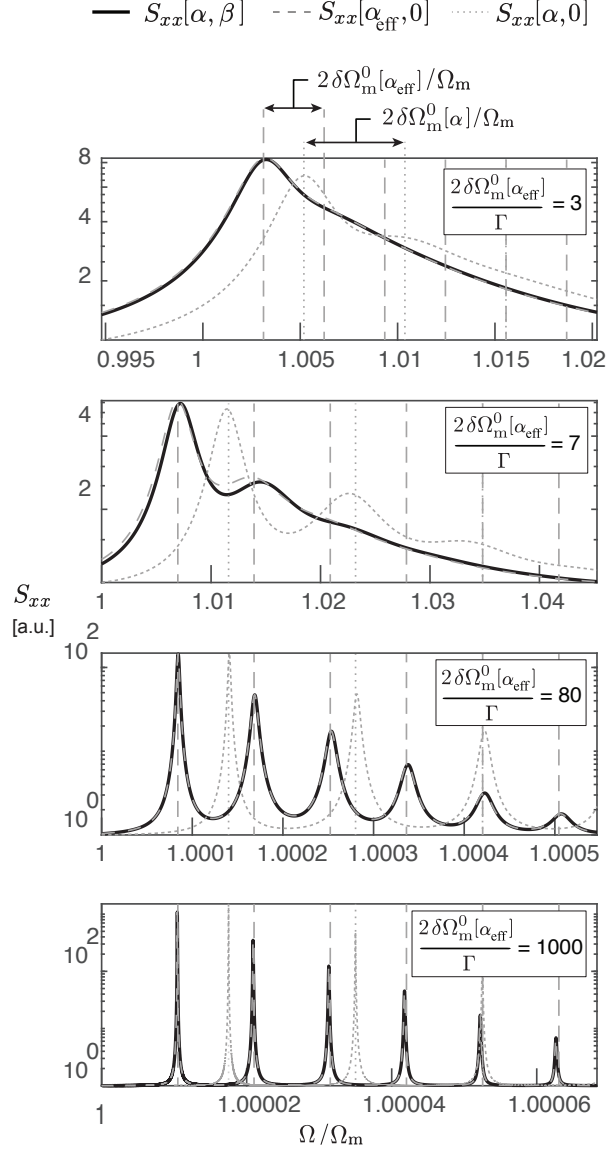


Figure 6: Numerically simulated spectra for the full master equation with a quartic Duffing ( $\alpha$ ) and cubic ( $\beta$ ) nonlinearity of the potential ( $S_{xx}[\alpha, \beta]$ , solid lines), the approximated model where the cubic nonlinearity manifests as a correction to the quartic Duffing strength ( $S_{xx}[\alpha_{\text{eff}}, 0]$ , dashed lines), and the spectra in absence of a cubic nonlinearity ( $S_{xx}[\alpha, 0]$ , dotted lines). Vertical lines at  $(E_{n+1} - E_n)/\hbar$  for  $n = 0, 1, 2, \dots$  indicate the analytic values of transition energies according to Eq. (21) with  $\delta\Omega_m^0[\alpha_{\text{eff}}]$  (dashed) and  $\delta\Omega_m^0[\alpha]$  (dotted). Input parameters:  $T = 50$  mK, and from top to bottom:  $R = 3$  nm,  $d = 5$  nm,  $Q = 1 \times 10^3$ ;  $R = 3$  nm,  $d = 25$  nm,  $Q = 1 \times 10^3$ ;  $R = 10$  nm,  $d = 5$  nm,  $Q = 1 \times 10^6$ ;  $R = 20$  nm,  $d = 5$  nm,  $Q = 1 \times 10^8$ .

## DISCUSSION

We have shown that third-sound resonances (surface oscillations of two-dimensional superfluid helium) are intrinsically strongly nonlinear, and we identified the specific parameters that allow one to maximize the nonlinearities: film thickness, confinement radius, and radial and rotational mode symmetry.

We predict that single-phonon nonlinear frequency shifts exceeding even those of graphene sheets and carbon nanotubes by orders of magnitude may be possible. Combined with the intrinsically low dissipation of motional states in superfluid [41], specifically when implemented in phononic crystal cavities [66], this may well open the door to the single-phonon nonlinear regime where a single phonon can shift the resonance frequency by more than the mechanical linewidth.

We presented the expected output spectrum in the presence of decoherence and showed that, in the near to mid quantum regime, a cubic nonlinearity can be treated analytically as an effective reduction of the quartic nonlinearity. Furthermore, we found that its reductive impact diminishes rapidly for surface waves with an increasing number of radial nodes.

The results dovetail recent theoretical proposals that lay out how strong Duffing nonlinearities can be used for quantum control and metrology [19, 24, 25, 27, 72, 73]. Ultimately, this would allow new tests of quantum macroscopicity and new tools for quantum technologies, where mechanical resonators can function not only as oscillators, memories, and interfaces, but also as qubits.

## ACKNOWLEDGEMENTS

This work was funded by the US Army Research Office through grant number W911NF17-1-0310 and the Australian Research Council Centre of Excellence for Engineered Quantum Systems (EQUS, project number CE170100009). W.P.B. and C.G.B. respectively acknowledge Australian Research Council Fellowships FT140100650 and DE190100318. L.T. is supported by the National Science Foundation (USA) under the Award No. 1720501.

## REFERENCES

- [1] Sletten, L. R., Moores, B. A., Viennot, J. J., and Lehnert, K. W. *Physical Review X* (2019).
- [2] Arrangoiz-Arriola, P., Wollack, E. A., Wang, Z., Pechal, M., Jiang, W., McKenna, T. P., Witmer, J. D., Van Laer, R., and Safavi-Naeini, A. H. *Nature* **571**(7766), 537–540 (2019).
- [3] Kues, M., Reimer, C., Roztock, P., Corts, L. R., Sciara, S., Wetzel, B., Zhang, Y., Cino, A., Chu, S. T., Little, B. E., Moss, D. J., Caspani, L., Azaa, J., and Morandotti, R. *Nature* **546**(7660), 622–626 June (2017).
- [4] Wang, C., Gao, Y. Y., Reinhold, P., Heeres, R. W., Ofek, N., Chou, K., Axline, C., Reagor, M., Blumoff, J., Sliwa, K. M., Frunzio, L., Girvin, S. M., Jiang, L., Mirrahimi, M., Devoret, M. H., and Schoelkopf, R. J. *Science* **352**(6289), 1087–1091 (2016).
- [5] Hensen, B., Bernien, H., Drau, A. E., Reiserer, A., Kalb, N., Blok, M. S., Ruitenber, J., Vermeulen, R. F. L., Schouten, R. N., Abelln, C., Amaya, W., Pruneri, V., Mitchell, M. W., Markham, M., Twitchen, D. J., Elkouss, D., Wehner, S., Taminiau, T. H., and Hanson, R. *Nature* **526**(7575), 682–686 October (2015).
- [6] Tian, L. *Physical Review Letters* **110**(23) (2013).
- [7] Hacker, B., Welte, S., Rempe, G., and Ritter, S. *Nature* **536**(7615), 193–196 August (2016).
- [8] Debnath, S., Linke, N. M., Figgatt, C., Landsman, K. A., Wright, K., and Monroe, C. *Nature* **536**(7614), 63–66 August (2016).
- [9] Arute, F., Arya, K., Babbush, R., Bacon, D., Bardin, J. C., Barends, R., Biswas, R., Boixo, S., Brandao, F. G. S. L., Buell, D. A., Burkett, B., Chen, Y., Chen, Z., Chiaro, B., Collins, R., Courtney, W., Dunsworth, A., Farhi, E., Foxen, B., Fowler, A., Gidney, C., Giustina, M., Graff, R., Guerin, K., Habegger, S., Harrigan, M. P., Hartmann, M. J., Ho, A., Hoffmann, M., Huang, T., Humble, T. S., Isakov, S. V., Jeffrey, E., Jiang, Z., Kafri, D., Kechedzhi, K., Kelly, J., Klimov, P. V., Knysh, S., Korotkov, A., Kostitsa, F., Landhuis, D., Lindmark, M., Lucero, E., Lyakh, D., Mandr, S., McClean, J. R., McEwen, M., Megrant, A., Mi, X., Michielsen, K., Mohseni, M., Mutus, J., Naaman, O., Neeley, M., Neill, C., Niu, M. Y., Ostby, E., Petukhov, A., Platt, J. C., Quintana, C., Rieffel, E. G., Roushan, P., Rubin, N. C., Sank, D., Satzinger, K. J., Smelyanskiy, V., Sung, K. J., Trevithick, M. D., Vainsencher, A., Villalonga, B., White, T., Yao, Z. J., Yeh, P., Zalcman, A., Neven, H., and Martinis, J. M. *Nature* **574**(7779), 505–510 October (2019).

- [10] Braginsky, V. B., Vorontsov, Y. I., and Thorne, K. S. *Science* **209**(4456), 547–557 (1980).
- [11] Thorne, K. S., Drever, R. W., Caves, C. M., Zimmermann, M., and Sandberg, V. D. *Physical Review Letters* **40**(11), 667 (1978).
- [12] Nakajima, T., Noiri, A., Yoneda, J., Delbecq, M. R., Stano, P., Otsuka, T., Takeda, K., Amaha, S., Allison, G., Kawasaki, K., et al. *Nature nanotechnology* **14**(6), 555–560 (2019).
- [13] Lei, C., Weinstein, A., Suh, J., Wollman, E., Kronwald, A., Marquardt, F., Clerk, A., and Schwab, K. *Physical review letters* **117**(10), 100801 (2016).
- [14] Kono, S., Koshino, K., Tabuchi, Y., Noguchi, A., and Nakamura, Y. *Nature Physics* **14**(6), 546–549 (2018).
- [15] Dayan, B., Parkins, A., Aoki, T., Ostby, E., Vahala, K., and Kimble, H. *Science* **319**(5866), 1062–1065 (2008).
- [16] Lemonde, M.-A., Didier, N., and Clerk, A. A. *Nature Communications* **7**(1), 11338 April (2016).
- [17] Guan, S., Bowen, W. P., Liu, C., and Duan, Z. *EPL (Europhysics Letters)* **119**(5), 58001 sep (2017).
- [18] Buluta, I., Ashhab, S., and Nori, F. *Reports on Progress in Physics* **74**(10), 104401 sep (2011).
- [19] Rips, S., Kiffner, M., Wilson-Rae, I., and Hartmann, M. J. *New Journal of Physics* (2012).
- [20] Rips, S., Wilson-Rae, I., and Hartmann, M. J. *Phys. Rev. A* **89**, 013854 Jan (2014).
- [21] Satzinger, K. J., Zhong, Y. P., Chang, H.-S., Peairs, G. A., Bienfait, A., Chou, M.-H., Cleland, A. Y., Conner, C. R., Dumur, ., Grebel, J., Gutierrez, I., November, B. H., Povey, R. G., Whiteley, S. J., Awschalom, D. D., Schuster, D. I., and Cleland, A. N. *Nature* **563**(7733), 661–665 November (2018).
- [22] Patil, Y. S., Chakram, S., Chang, L., and Vengalattore, M. *Phys. Rev. Lett.* **115**, 017202 Jun (2015).
- [23] Greywall, D. S., Yurke, B., Busch, P. A., Pargellis, A. N., and Willett, R. L. *Phys. Rev. Lett.* **72**, 2992–2995 May (1994).
- [24] Babourina-Brooks, E., Doherty, A., and Milburn, G. J. *New Journal of Physics* **10** (2008).
- [25] Woolley, M. J., Milburn, G. J., and Caves, C. M. *New Journal of Physics* **10** (2008).
- [26] Szorkovszky, A., Doherty, A. C., Harris, G. I., and Bowen, W. P. *Physical review letters* **107**(21), 213603 (2011).
- [27] Lü, X.-Y., Liao, J.-Q., Tian, L., and Nori, F. *Physical Review A* **91**, 13834 (2015).
- [28] Szorkovszky, A., Brawley, G. A., Doherty, A. C., and Bowen, W. P. *Physical Review Letters* (2013).
- [29] Warszawski, P., Szorkovszky, A., Bowen, W. P., and Doherty, A. C. *New Journal of Physics* **21**(2), 023020 feb (2019).
- [30] Rips, S. and Hartmann, M. J. *Phys. Rev. Lett.* **110**, 120503 Mar (2013).
- [31] Antoni, Thomas, Makles, Kevin, Braive, Rémy, Briant, Tristan, Cohadon, Pierre-François, Sagnes, Isabelle, Robert-Philip, Isabelle, and Heidmann, Antoine. *EPL* **100**(6), 68005 (2012).
- [32] Lee, S. I., Howell, S. W., Raman, A., and Reifenger, R. *Physical Review B - Condensed Matter and Materials Physics* **66**(11), 1–10 (2002).
- [33] Maillet, O., Zhou, X., Gazizulin, R. R., Ilic, R., Parpia, J. M., Bourgeois, O., Fefferman, A. D., and Collin, E. *ACS Nano* **12**(6), 5753–5760 06 (2018).
- [34] Hocke, F., Pernpeintner, M., Zhou, X., Schliesser, A., Kippenberg, T. J., Huebl, H., and Gross, R. *Applied Physics Letters* **105**(13), 133102 2020/01/22 (2014).
- [35] Suh, J., Lahaye, M. D., Echternach, P. M., Schwab, K. C., and Roukes, M. L. *Nano Letters* **10**(10), 3990–3994 (2010).
- [36] Eichler, A., Moser, J., Chaste, J., Zdrojek, M., Wilson-Rae, I., and Bachtold, A. *Nature Nanotechnology* **6**(6), 339–342 (2011).
- [37] Huang, P., Zhou, J., Zhang, L., Hou, D., Lin, S., Deng, W., Meng, C., Duan, C., Ju, C., Zheng, X., Xue, F., and Du, J. *Nature Communications* **7** (2016).
- [38] Harris, G. I., McAuslan, D. L., Sheridan, E., Sachkou, Y., Baker, C., and Bowen, W. P. *Nat Phys* **12**(8), 788–793 08 (2016).

- [39] He, X., Harris, G. I., Baker, C. G., Sawadsky, A., Sfindla, Y. L., Sachkou, Y. P., Forstner, S., and Bowen, W. P. *Nature Physics* (2020).
- [40] Sachkou, Y. P., Baker, C. G., Harris, G. I., Stockdale, O. R., Forstner, S., Reeves, M. T., He, X., McAuslan, D. L., Bradley, A. S., Davis, M. J., and Bowen, W. P. *Science* **366**(6472), 1480–1485 December (2019).
- [41] Ellis, F. M. and Luo, H. *Phys. Rev. B* **39**, 2703–2706 Feb (1989).
- [42] McAuslan, D. L., Harris, G. I., Baker, C., Sachkou, Y., He, X., Sheridan, E., and Bowen, W. P. *Phys. Rev. X* **6**, 021012 Apr (2016).
- [43] Hoffmann, J. A., Penanen, K., Davis, J. C., and Packard, R. E. *Journal of Low Temperature Physics* **135**(3), 177–202 (2004).
- [44] Ellis, F. M. and Hallock, R. B. *Review of Scientific Instruments* **54**(6), 751–753 jun (1983).
- [45] Lifshitz, R. and Cross, M. C. In *Reviews of Non-linear Dynamics and Complexity*, 1–52. (2009).
- [46] Nayfeh, A. H. and Mook, D. T. *Nonlinear Oscillations*. Wiley Classics Library. Wiley, (2008).
- [47] Kozinsky, I., Postma, H. W., Bargatin, I., and Roukes, M. L. *Applied Physics Letters* **88**(25) (2006).
- [48] Lorenzo, L. A. D. and Schwab, K. C. *New Journal of Physics* **16**(11), 113020 nov (2014).
- [49] Childress, L., Schmidt, M. P., Kashkanova, A. D., Brown, C. D., Harris, G. I., Aiello, A., Marquardt, F., and Harris, J. G. *Physical Review A* (2017).
- [50] Shkarin, A. B., Kashkanova, A. D., Brown, C. D., Garcia, S., Ott, K., Reichel, J., and Harris, J. G. *Physical Review Letters* (2019).
- [51] Kashkanova, A. D., Shkarin, A. B., Brown, C. D., Flowers-Jacobs, N. E., Childress, L., Hoch, S. W., Hohmann, L., Ott, K., J Reichel, and Harris, J. G. E. *Journal of Optics* **19**(3), 034001 (2017).
- [52] Kashkanova, A. D., Shkarin, A. B., Brown, C. D., Flowers-Jacobs, N. E., Childress, L., Hoch, S. W., Hohmann, L., Ott, K., Reichel, J., and Harris, J. G. *Nature Physics* **13**(1), 74–79 (2017).
- [53] Rojas, X. and Davis, J. P. *Physical Review B - Condensed Matter and Materials Physics* (2015).
- [54] Souris, F., Rojas, X., Kim, P. H., and Davis, J. P. *Physical Review Applied* **7**(4) (2017).
- [55] Forstner, S., Sachkou, Y., Woolley, M., Harris, G. I., He, X., Bowen, W. P., and Baker, C. G. *New Journal of Physics* **21**(5), 053029 may (2019).
- [56] Ellis, F. M. and Li, L. *Phys. Rev. Lett.* **71**, 1577–1580 Sep (1993).
- [57] Schechter, A. M. R., Simmonds, R. W., Packard, R. E., and Davis, J. C. *Nature* **396**(6711), 554–557 (1998).
- [58] Baker, C. G., Harris, G. I., McAuslan, D. L., Sachkou, Y., He, X., and Bowen, W. P. *New Journal of Physics* **18**(12), 123025 dec (2016).
- [59] Tilley, D. R. and Tilley, J. *Superfluidity and Superconductivity*. Graduate Student Series in Physics. Taylor & Francis, (1990).
- [60] Atkins, K. R. *Physical Review* **113**(4), 962–965 (1959).
- [61] Olver, F. *Royal Society Mathematical Tables: Volume 7, Bessel Functions, Part 3, Zeros and Associated Values*. Cambridge University Press, (1960).
- [62] Bowen, W. P. and Milburn, G. J. *Quantum Optomechanics*. Taylor & Francis, (2015).
- [63] Ricci, F., Rica, R. A., Spasenović, M., Gieseler, J., Rondin, L., Novotny, L., and Quidant, R. *Nature Communications* **8**(1), 15141 (2017).
- [64] Gil-Santos, E., Baker, C., Nguyen, D. T., Hease, W., Gomez, C., Lemaître, A., Ducci, S., Leo, G., and Favero, I. *Nature Nanotechnology* **10**(9), 810–816 September (2015).
- [65] Descharmes, N., Dharanipathy, U. P., Diao, Z., Tonin, M., and Houdré, R. *Lab on a Chip* **13**(16), 3268–3274 (2013).
- [66] Condat, C. A. and Kirkpatrick, T. R. *Physical Review B* **32**(7), 4392 (1985).
- [67] Setter, A., Vovrosh, J., and Ulbricht, H. *Applied Physics Letters* **115**(15), 153106 (2019).
- [68] Matheny, M. H., Villanueva, L. G., Karabalin, R. B., Sader, J. E., and Roukes, M. L. *Nano Letters* **13**(4), 1622–1626 04 (2013).

- [69] Sansa, M., Sage, E., Bullard, E. C., Gély, M., Alava, T., Colinet, E., Naik, A. K., Villanueva, L. G., Duraffourg, L., Roukes, M. L., Jourdan, G., and Hentz, S. *Nature Nanotechnology* **11**(6), 552–558 (2016).
- [70] Chan, H. B., Aksyuk, V. A., Kleiman, R. N., Bishop, D. J., and Capasso, F. *Physical Review Letters* **87**(21), 211801–1–211801–4 (2001).
- [71] Sabisky, E. S. and Anderson, C. H. *Phys. Rev. A* **7**, 790–806 Feb (1973).
- [72] Buks, E. and Yurke, B. *Physical Review E - Statistical, Nonlinear, and Soft Matter Physics* (2006).
- [73] Momeni, F. and Naderi, M. H. *Journal of the Optical Society of America B* (2019).

# Supplementary Information: Extreme quantum nonlinearity in superfluid thin-film surface waves

Yasmine L. Sfendla<sup>1</sup>, Christopher G. Baker<sup>1</sup>, Glen I. Harris<sup>1</sup>, Lin Tian<sup>2</sup>, and Warwick P. Bowen<sup>1</sup>

<sup>1</sup>*ARC Centre of Excellence for Engineered Quantum Systems, School of Mathematics and Physics, The University of Queensland, Brisbane 4072, Australia*

<sup>2</sup>*School of Natural Sciences, University of California, Merced, California 95343, USA*

(Dated: May 28, 2020)

## I. Nonlinear spring constants for a superfluid thin film

As detailed in the main text, the linear spring constant  $k$ , cubic nonlinearity  $\beta$  and quartic (Duffing) nonlinearity  $\alpha$  for a superfluid surface wave of amplitude  $\eta[r, \theta]$  are given by

$$k = \frac{3\rho a_{\text{vdw}}}{d^4} \int_0^{2\pi} \int_0^R \frac{\eta^2[r, \theta]}{\eta^2[R, 0]} r \, dr \, d\theta, \quad (1)$$

$$\beta = -\frac{6\rho a_{\text{vdw}}}{d^5} \int_0^{2\pi} \int_0^R \frac{\eta^3[r, \theta]}{\eta^3[R, 0]} r \, dr \, d\theta \quad (2)$$

and

$$\alpha = \frac{10\rho a_{\text{vdw}}}{d^6} \int_0^{2\pi} \int_0^R \frac{\eta^4[r, \theta]}{\eta^4[R, 0]} r \, dr \, d\theta. \quad (3)$$

In order to reveal the explicit dependence of the (non)linear spring constants on  $R$ ,  $d$ ,  $\mu$  and  $\nu$ , we evaluate the integrals further.

The integrals in equations (1–3) can be written jointly as a function  $\Phi_{\mu, \nu}^{(p)}$  with  $p = 2, 3$  and 4, with

$$\Phi_{\mu, \nu}^{(p)} := \int_0^{2\pi} \int_0^R \frac{J_\mu^p[\zeta_{\mu, \nu} \frac{r}{R}] \cos^p(\mu\theta)}{J_\mu^p[\zeta_{\mu, \nu}]} r \, dr \, d\theta. \quad (4)$$

The integral over the angular coordinate  $\theta$  in Eq. (4) is

$$\int_0^{2\pi} \cos^p(\mu\theta) \, d\theta = 2\pi \left( \delta_{\mu 0} + (1 - \delta_{\mu 0})(1 - \delta_{p3}) \frac{(p-1)!!}{p!!} \right) \quad (5)$$

$$= \left\{ \pi(1 + \delta_{\mu 0}), 2\pi\delta_{\mu 0}, \pi \frac{3 + 5\delta_{\mu 0}}{4} \right\} \text{ for } p = \{2, 3, 4\}, \quad (6)$$

where we have introduced the Kronecker delta function  $\delta$ . Observe here: the reduction of this integral to  $2\pi\delta_{\mu 0}$  for  $p = 3$  implies that  $\Phi_{\mu \neq 0, \nu}^{(3)} = 0$ , so the cubic

nonlinearity  $\beta$  vanishes for all but the zeroth-order ( $\mu = 0$ ) superfluid modes.

We can rewrite the remainder of Eq. (4) by substitution of the integrand:

$$\begin{aligned} J_\mu^{-p}[\zeta_{\mu, \nu}] \int_0^R J_\mu^p\left[\zeta_{\mu, \nu} \frac{r}{R}\right] r \, dr \\ = \frac{\int_0^{\zeta_{\mu, \nu}} J_\mu^p[q] q \, dq}{\zeta_{\mu, \nu}^2 J_\mu^p[\zeta_{\mu, \nu}]} R^2 \\ := \phi_{\mu, \nu}^{(p)} R^2. \end{aligned} \quad (7)$$

It follows immediately that all spring constants  $k$ ,  $\beta$  and  $\alpha$  scale with the square of the confinement radius:

$$\Phi_{\mu, \nu}^{(p)} = 2\pi \left( \delta_{\mu 0} + (1 - \delta_{\mu 0})(1 - \delta_{p3}) \frac{(p-1)!!}{p!!} \right) \phi_{\mu, \nu}^{(p)} R^2. \quad (8)$$

The constants  $\phi_{\mu, \nu}^{(p)} = \frac{\int_0^{\zeta_{\mu, \nu}} J_\mu^p[q] q \, dq}{\zeta_{\mu, \nu}^2 J_\mu^p[\zeta_{\mu, \nu}]}$  are tabulated in Table 1 for the three lowest mode orders  $\mu$  and  $\nu$ .

It is worth noting here that for  $p = 2$ , i.e., for the spring constant  $k$ , a closed-form expression exists for the integral  $\int_0^{\zeta_{\mu, \nu}} J_\mu^2[q] q \, dq$ . In that case, we find

$$\begin{aligned} \int_0^{\zeta_{\mu, \nu}} J_\mu^2[q] q \, dq &= \frac{\zeta_{\mu, \nu}^2}{2} (J_{\mu-1}^2[\zeta_{\mu, \nu}] + J_\mu^2[\zeta_{\mu, \nu}]) \\ &\quad - \mu \zeta_{\mu, \nu} J_{\mu-1}[\zeta_{\mu, \nu}] J_\mu[\zeta_{\mu, \nu}] \\ &= \frac{\zeta_{\mu, \nu}^2 - \mu^2}{2} J_\mu^2[\zeta_{\mu, \nu}], \end{aligned}$$

where we took advantage of the Bessel function recurrence relations and our definition  $J'_\mu[\zeta_{\mu, \nu}] = 0$  so that  $J_{\mu-1}[\zeta_{\mu, \nu}] = \frac{\mu}{\zeta_{\mu, \nu}} J_\mu[\zeta_{\mu, \nu}]$ . Then,

$$\phi_{\mu, \nu}^{(2)} = \frac{1}{2} \left( 1 - \frac{\mu^2}{\zeta_{\mu, \nu}^2} \right). \quad (9)$$

Since  $\zeta_{\mu, \nu}$  is always larger than  $\mu$ , we have

$$0 < \phi_{\mu, \nu}^{(2)} \leq \frac{1}{2} \quad (10)$$

and up to first order  $\phi_{\mu,\nu}^{(2)}$  is independent of  $\mu$  and  $\nu$ . While no closed form exists for  $\phi_{\mu,\nu}^{(3)}$ , it too, is found to be bounded:

$$0 < |\phi_{\mu,\nu}^{(3)}| \leq |\phi_{0,1}^{(3)}| = 0.44. \quad (11)$$

The function  $\phi_{\mu,\nu}^{(4)}$  does not converge for  $\nu \rightarrow \infty$ , but it grows sufficiently slowly that for the first twenty mode numbers it is contained in a relatively small interval:

$$0 < \phi_{\mu,\nu}^{(4)} \leq \phi_{0,20}^{(4)} = 2.3 \quad (\mu, \nu \leq 20). \quad (12)$$

The observations (10–12) are important, because the (non)linear spring constants depend on the mode numbers  $\mu$  and  $\nu$  through the function  $\phi_{\mu,\nu}^{(p)}$ .

$\phi_{\mu,\nu}^{(2)}$			
	$\nu = 1$	$\nu = 2$	$\nu = 3$
$\mu = 0$	1/2	1/2	1/2
$\mu = 1$	0.353	0.482	0.493
$\mu = 2$	0.286	0.456	0.480
$\phi_{\mu,\nu}^{(3)}$			
$\mu = 0$	-0.437	0.259	-0.236
$\phi_{\mu,\nu}^{(4)}$			
$\mu = 0$	1.28	1.48	1.61
$\mu = 1$	0.290	0.837	1.03
$\mu = 2$	0.223	0.704	0.891

Table 1: Coefficients  $\phi_{\mu,\nu}^{(p)} = \frac{\int_0^{\zeta_{\mu,\nu}} J_\mu^p[q] q dq}{\zeta_{\mu,\nu}^2 J_\mu^p[\zeta_{\mu,\nu}]}$  for  $p = \{2, 3, 4\}$  with  $\zeta_{\mu,\nu}$  the  $\nu^{\text{th}}$  zero of  $J_\mu'$ .

With Eq. (4), (8) and (9), we can then expose the dependence of the (non)linear spring constants on the film thickness  $d$  and confinement radius  $R$ :

$$k = (1 + \delta_{\mu 0}) 3\pi \rho a_{\text{vdw}} \phi_{\mu,\nu}^{(2)} \frac{R^2}{d^4} \quad (13)$$

$$= (1 + \delta_{\mu 0}) \frac{3\pi}{2} \rho a_{\text{vdw}} \left(1 - \frac{\mu^2}{\zeta_{\mu,\nu}^2}\right) \frac{R^2}{d^4}, \quad (14)$$

$$\beta = -\delta_{\mu 0} 12\pi \rho a_{\text{vdw}} \phi_{0,\nu}^{(3)} \frac{R^2}{d^5} \quad (15)$$

and

$$\alpha = (3 + 5\delta_{\mu 0}) \frac{5\pi}{2} \rho a_{\text{vdw}} \phi_{\mu,\nu}^{(4)} \frac{R^2}{d^6}. \quad (16)$$

## II. Spectral function calculation with Lindblad master equation

We numerically solve the spectral function of the nonlinear resonator, using the full Lindblad master equation of the open quantum system comprising the resonator and its environment.

The Hamiltonian of the nonlinear mechanical mode  $H = \frac{p^2}{2m_{\text{eff}}} + \frac{1}{2}kx^2 + \frac{1}{3}\beta x^3 + \frac{1}{4}\alpha x^4$  can be written in terms of the eigenstates  $|j\rangle$  and eigenvalues  $E_j$  as  $H = \sum_j E_j |j\rangle\langle j|$ . The eigenstates and eigenvalues are obtained by numerically discretizing and diagonalizing the Hamiltonian. The oscillation amplitude can be written in terms of the eigenbasis as

$$x = \sum_{k>j} (x_{jk} |j\rangle\langle k| + \text{h.c.}) + \sum_j x_{jj} |j\rangle\langle j|, \quad (17)$$

with matrix elements  $x_{jk} = \langle j|x|k\rangle$ . The quantum master equation of the mechanical mode coupled to a bath of environmental modes can be derived using the standard perturbation theory approach in the eigenbasis [1]. Omitting the fast rotating terms in the system-bath coupling, we obtain the Lindblad master equation:

$$\frac{d\rho}{dt} = -i[H, \rho] + \mathcal{L}\rho \quad (18)$$

with

$$\mathcal{L} = \frac{\Gamma}{2} \sum_{k>j} |x_{jk}|^2 \left( (n_{\text{th}}[\delta E_{kj}] + 1) \mathcal{D}_{jk} + n_{\text{th}}[\delta E_{kj}] \mathcal{D}_{kj} \right), \quad (19)$$

where  $\rho$  is the density matrix of the mechanical mode,  $n_{\text{th}}[\delta E_{kj}] = (e^{\hbar\delta E_{kj}/k_B T} - 1)^{-1}$  is the thermal phonon occupation number at temperature  $T$  for the frequency difference  $\delta E_{kj} = E_k - E_j$  between the states  $k$  and  $j$ , and

$$\mathcal{D}_{jk} \rho = 2 |j\rangle\langle k| \rho |k\rangle\langle j| - |k\rangle\langle k| \rho - \rho |k\rangle\langle k| \quad (20)$$

is the Lindblad superoperator for the jump operation  $|j\rangle\langle k|$ . The difference between Eq. (18) and the standard master equation for a quantum harmonic oscillator stems from the nonlinearity in the Hamiltonian, which perturbs the equal energy level spacing.

Defining amplitude operators  $\epsilon^+ = \sum_{k>j} x_{jk} |j\rangle\langle k|$  and  $\epsilon^- = (\epsilon^+)^{\dagger}$ , one can calculate the correlation function  $G[\tau]$  of the mechanical amplitude as a function of the separation time  $\tau$ :

$$G[\tau] = \langle \epsilon^- [t + \tau] \epsilon^+ [t] \rangle_{t \rightarrow \infty}. \quad (21)$$

Here we used the Heisenberg representation for the time-dependent operator  $\epsilon$  such that  $\epsilon[t] =$



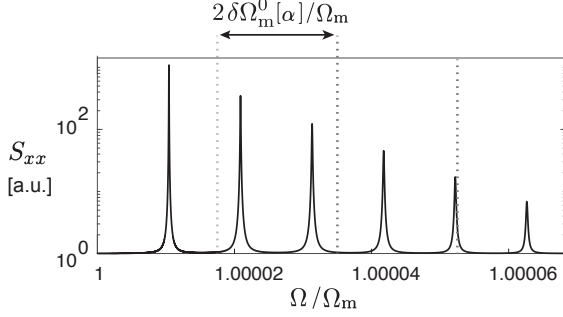


Figure 1: Numerically simulated spectrum of the mechanical oscillator in the presence of decoherence for a  $R = 20$  nm,  $d = 5$  nm,  $Q = 1 \times 10^8$ , ( $\mu = 0$ ;  $\nu = 1$ ) third-sound mode at  $T = 50$  mK with resulting (non)linear spring constants  $k = 2 \times 10^{-3}$  N m $^{-1}$ ,  $\beta = 8 \times 10^5$  N m $^{-2}$  and  $\alpha = 8 \times 10^{14}$  N m $^{-3}$ . Vertical lines at  $(E_{n+1} - E_n)/\hbar$  for  $n = 0, 1, 2, \dots$  represent the analytic values of transition energies according to first-order perturbation theory, separated by the single-phonon nonlinear shift  $2\delta\Omega_m^0[\alpha]$ .

$e^{i\tilde{H}t} \epsilon e^{-i\tilde{H}t}$  with  $\tilde{H}$  the total Hamiltonian of the mechanical mode coupled to the bath modes.

Applying the quantum regression theorem [2], we write the correlation in Eq. (21) as a trace over the Hilbert space of the mechanical mode. In doing so, we introduce the stationary density matrix of the master equation (18)  $\varrho_{ss}$ , which is obtained by setting  $\frac{d\varrho}{dt} = 0$  in Eq. (19). The correlation function then becomes:

$$G[\tau] = \text{Tr}_s [\epsilon^- e^{\mathcal{L}\tau} (\epsilon^+ \varrho_{ss})]. \quad (22)$$

These equations are implemented numerically [3] to find the solution of  $G[\tau]$ . The spectral function  $S_{xx}[\Omega]$  can then be obtained as the Fourier transformation of  $G[\tau]$ :

$$S_{xx}[\Omega] = \frac{1}{2\pi} \int_{-\infty}^{\infty} e^{-i\Omega\tau} G[\tau] d\tau. \quad (23)$$

A resulting correlation spectrum in the single-phonon nonlinear regime is shown in Fig. 1 for system parameters corresponding to a  $R = 20$  nm,  $d = 5$  nm, ( $\mu = 0$ ;  $\nu = 1$ ) third-sound mode. Manifestly, single-phonon transitions are spectrally resolved. With vertical lines we have indicated the transition frequencies  $\Omega[n] = \frac{E_{n+1} - E_n}{\hbar} = \Omega_m + 2(n+1)\delta\Omega_m^0$ , predicted from the first-order (i.e., pure Duffing) analytical approximation. It can be seen that the single-phonon nonlinear shift  $2\delta\Omega_m^0[\alpha]$  agrees rather poorly with the one predicted for the pure Duffing nonlinear resonator. The reason is that the first-order approximation excludes the cubic potential term. Its effect is investigated in Section IV in the main text.

## References

- [1] Gardiner, C. and Zoller, P. *Quantum Noise*. Springer Series in Synergetics. Springer, 3 edition, (2004).
- [2] Lax, M. *Phys. Rev.* **129**, 2342–2348 Mar (1963).
- [3] Tan, S. M. *Journal of Optics B: Quantum and Semiclassical Optics* **1**(4), 424–432 aug (1999).